

Orthogonality of Separation in Two-Dimensional Liquid Chromatography

Martin Gilar,* Petra Olivova, Amy E. Daly, and John C. Gebler

Waters Corporation, 34 Maple Street, Milford, Massachusetts 01757

Two-dimensional liquid chromatography is often used to reduce the proteomic sample complexity prior to tandem mass spectrometry analysis. The 2D-LC performance depends on the peak capacity in both chromatographic dimensions, and separation orthogonality. The peak capacity and selectivity of many LC modes for peptides is not well known, and mathematical characterization for orthogonality is underdeveloped. Consequently, it is difficult to estimate the performance of 2D-LC for peptide separation. The goal of this paper was to investigate a selectivity of common LC modes and to identify the 2D-LC systems with a useful orthogonality. A geometric approach for orthogonality description was developed and applied for estimation of a practical peak 2D-LC capacity. Selected LC modes including various RP, SCX, SEC, and HILIC were combined in 2D-LC setups. SCX-RP, HILIC-RP, and RP-RP 2D systems were found to provide suitable orthogonality. The RP-RP system (employing significantly different pH in both RP separation dimensions) had the highest practical peak capacity of 2D-LC systems investigated.

Current proteome research involves the analysis of greatly complex samples, often comprising hundreds of thousands of proteins or peptides.^{1–5} Despite the recent progress in column and instrument technology, the separation performance of liquid chromatography (LC) is not sufficient to adequately resolve sample constituents within a single analysis.^{6,7} Two-dimensional liquid chromatography (2D-LC) has been applied to improve the separation and reduce the sample complexity to an acceptable level prior to tandem mass spectrometry (MS/MS) analysis.⁸

Because both LC separation and MS identification of intact proteins is difficult, the LC–MS analysis is typically performed on a peptide level, after protein digestion with suitable proteolytic enzymes. This further increases the sample complexity and reinforces the demands for efficient separation methods.

The separation efficiency of HPLC under gradient conditions is best described by a peak capacity (P), which represents the maximum number of components that could be theoretically separated on a given LC column within a gradient time (t_g).^{9–11} State-of-the-art reversed-phase (RP)-LC columns provide a peak capacity of several hundreds, depending on their length and the gradient slope. A recent study outlines three strategies for LC peak capacity improvements:¹² (i) decreasing the gradient slope (column length is fixed), (ii) increasing the column length (L) with proportional increase in gradient time, and (iii) employing columns packed with smaller sorbent particles. Because the gains in peak capacity are not linear with the increase of t_g and L , the first two strategies have diminishing returns. The third strategy is limited by the operational pressure. A predicted maximum achievable peak capacity in single-dimensional (1D) RP-LC is within the range of 1400–1600.¹²

The attractiveness of 2D-LC lays in its potential to dramatically improve the separation power of chromatography. Peak capacity for 2D separation is defined as a linear combination of peak capacities in both separation dimension;¹³ for example, when combining orthogonal LC modes with the peak capacities of 50 and 100, the resulting 2D capacity should be 5000. In reality, the 2D-LC performance depends also on the orthogonality LC modes. If the selectivity of the two LC modes is not completely orthogonal (dissimilar), the achievable peak capacity is lower than expected.

Only a limited number of studies investigated the concept of orthogonality in 2D-LC for peptide separation.^{14–16} The most common 2D-LC setup employs a combination of strong cation exchange (SCX) chromatography with RP-LC. Current reports

* Corresponding author. Tel: +1 508 482 2000. Fax: +1 508 482 3100. E-mail: Martin_Gilar@waters.com.

- (1) Washburn, M. P.; Wolters, D.; Yates, J. R., 3rd. *Nat. Biotechnol.* **2001**, *19*, 242–247.
- (2) Wagner, K.; Miliotis, T.; Marko-Varga, G.; Bischoff, R.; Unger, K. K. *Anal. Chem.* **2002**, *74*, 809–820.
- (3) Peng, J.; Elias, J. E.; Thoreen, C. C.; Licklider, L. J.; Gygi, S. P. *J. Proteome Res.* **2003**, *2*, 43–50.
- (4) Kachman, M. T.; Wang, H.; Schwartz, D. R.; Cho, K. R.; Lubman, D. M. *Anal. Chem.* **2002**, *74*, 1779–1791.
- (5) Silva, J. C.; Denny, R.; Dorschel, C. A.; Gorenstein, M.; Kass, I. J.; Li, G. Z.; McKenna, T.; Nold, M. J.; Richardson, K.; Young, P.; Geromanos, S. *Anal. Chem.* **2005**, *77*, 2187–2200.
- (6) Tolley, L.; Jorgenson, J. W.; Moseley, M. A. *Anal. Chem.* **2001**, *73*, 2985–2991.
- (7) Shen, Y.; Jacobs, J. M.; Camp, D. G., 2nd; Fang, R.; Moore, R. J.; Smith, R. D.; Xiao, W.; Davis, R. W.; Tompkins, R. G.; Zhao, R.; Berger, S. J.; Anderson, G. A.; Rodriguez, N. *Anal. Chem.* **2004**, *76*, 1134–1144.

- (8) Wehr, T. *LCGC North Am.* **2002**, *20*, 954–962.
- (9) Stadalius, M. A.; Ghrist, B. F.; Snyder, L. R. *J. Chromatogr.* **1987**, *387*, 21–40.
- (10) Ghrist, B. F.; Stadalius, M. A.; Snyder, L. R. *J. Chromatogr.* **1987**, *387*, 1–19.
- (11) Neue, U. D.; Carmody, J. L.; Cheng, Y. F.; Lu, Z.; Phoebe, C. H.; Wheat, T. E. *Design of rapid gradient methods for the analysis of combinatorial chemistry libraries and the preparation of pure compound*; Marcel Dekker: New York, 2001.
- (12) Gilar, M.; Daly, A. E.; Kele, M.; Neue, U. D.; Gebler, J. C. *J. Chromatogr., A* **2004**, *1061*, 183–192.
- (13) Giddings, J. C. *J. High Resolut. Chromatogr.* **1987**, *10*, 319–323.
- (14) Liu, Z.; Patterson, D. G.; Lee, M. L. *Anal. Chem.* **1995**, *67*, 3840–3845.
- (15) Slonecker, P. J.; Li, X.; Ridgway, T. H.; Dorsey, J. G. *Anal. Chem.* **1996**, *68*, 682–689.
- (16) Giddings, J. C. *J. Chromatogr., A* **1995**, *703*, 3–15.

indicate that SCX-RP separation modes are not completely orthogonal.^{2,3,17} In principle, the retention in SCX mode is driven by the solute charge. Since the tryptic peptides are mostly 2+ (arginine/lysine at C terminal plus primary amine at N terminal), or 3+ charged (additional charge is due to histidine in the sequence), the majority of them cluster within a relatively narrow elution window. The remaining parts of the chromatogram are only sparsely populated by the 1+, 4+, and 5+ charged peptides.¹⁷

Other LC separation modes were used for 2D-LC; however, their mutual orthogonality has not been fully investigated. In rare cases when the experimental data are available, the lack of adequate mathematical methods makes it difficult to characterize the degree of orthogonality of achieved 2D separations.^{2,3}

Among the few systematic approaches, Slonecker et al.^{15,18} developed methods for describing the independence of separation modes using the tools of informational theory. The authors used the informational similarity (IS) and percentage of synentropy (PS) for the description of data scatter in 2D separation space. The IS defines the degree of data overlap (or the solute crowding in the separation space), while PS is a measure of the percentage of 2D informational entropy. The authors used additional descriptors, such as peak spreading angle and practical peak capacity, (N_p) introduced earlier by Liu et al.¹⁴ The Liu geometric approach is based on the factor analysis and correlation matrixes. The authors defined the orthogonality using the effective area of 2D separation space covered by the eluting peaks. The practical peak capacity is then calculated as the theoretical peak capacity multiplied by the fraction of area. Despite considerable effort, both mathematical approaches have some limitations. First, multiple descriptors are used to define the orthogonality. Second, the proposed methods may not satisfactorily describe the orthogonality for the situations (2D modes) where the analytes are not distributed diagonally along the 2D separation space but form several distinct clusters not intersecting the diagonal (e.g., the case of SCX-RP 2D-LC).¹⁷

The goal of this work was to evaluate the selectivity of several LC modes and consequently identify the most suitable systems for 2D-LC of peptides. We focused on the LC methods utilizing mobile phases that are directly compatible with MS detection, namely, the RP, hydrophilic interaction chromatography (HILIC), size exclusion chromatography (SEC), and SCX (using volatile mobile phases). The orthogonality and practical peak capacity of multiple 2D-LC modes were compared. A new geometric approach is proposed for the characterization of separation orthogonality.

EXPERIMENTAL SECTION

Materials and Reagents. Formic acid (FA) was purchased from Sigma-Aldrich (St. Louis, MO). HPLC grade acetonitrile and ammonium hydroxide were purchased from J.T. Baker (Phillipsburg, NJ). A Milli-Q system (Millipore, Bedford, MA) was used to prepare deionized water (18 M Ω cm) for HPLC mobile phases. MassPREP protein tryptic digestion standards of enolase, ADH, phosphorylase *b*, hemoglobin, and BSA were obtained from Waters (Milford, MA). MassPREP peptide standard (containing additional seven nontryptic peptides) was obtained from the same source.

LC–UV–MS Instrumentation, Columns, and Conditions. LC–MS experiments were carried out using the following instru-

ments: model 2796 Alliance Bio HPLC system with a 996 photodiode array detector (micro UV cell) connected on-line to a single quadrupole Micromass ZQ 4000 MS instrument (all Waters). The 150 \times 2.1 mm RP columns were packed with the following chromatographic sorbents: Atlantis dC₁₈, 3 μ m; XTerra Phenyl, 3.5 μ m; XTerra MS C₁₈, 3.5 μ m; pentafluorophenyl (PFP), 5 μ m (Waters). SEC column 250 \times 4.6 mm was packed with YMC diol sorbent, 60- \AA , 5 μ m (Waters). The 150 \times 2.1 mm SCX column was packed with Polysulfoethyl A, 5- μ m, 300- \AA sorbent, which was purchased from PolyLC Inc. (Columbia, MD).

RP experiments with dC₁₈ and Phenyl columns were carried out as follows: Mobile phase A was 0.2% FA in water, pH 2.6, and B was 0.16% FA in acetonitrile; flow rate was 0.2 mL/min. The gradient was 0.8% acetonitrile/min, separation temperature 40 $^{\circ}$ C. RP experiment at high pH was run with hybrid silica column XTerra MS C₁₈. Mobile phase A was water, B acetonitrile, and C 200 mM ammonium formate (NH₄FA) aqueous buffer; pH 10. Flow rate was 0.2 mL/min, separation temperature 40 $^{\circ}$ C. The gradient was 0.8% acetonitrile/min; pump C was used to deliver isocratically 10% of solvent, so the mobile phase contained a constant concentration of 20 mM NH₄FA buffer. The buffer was prepared by adding 12.5 g of concentrated ammonium hydroxide (28% aqueous solution) into 900 mL of water and 1.62 mL of FA (99%). The pH was adjusted with ammonium hydroxide or FA to pH 10, and the volume was brought to 1 L. The RP experiment using the PFP column was as follows: Mobile phase A was water, B acetonitrile, and C 400 mM NH₄FA aqueous buffer; pH 3.25. Flow rate was 0.2 mL/min, separation temperature 40 $^{\circ}$ C. The gradient was 0.8% acetonitrile/min; pump C was used to deliver isocratically 20% solvent, so the mobile phase contained a constant concentration of 80 mM NH₄FA buffer. The buffer was prepared by adding 24.7 g of concentrated ammonium hydroxide (28% aqueous solution) into 900 mL of water and 50 mL of FA (99%). The pH was adjusted either with ammonium hydroxide or FA to pH 3.25, and the volume was brought to 1 L. The SEC experiment was carried out using three 250 \times 4.6 mm columns connected serially. Mobile phase was mixed using pumps: Mobile phase A was water, B acetonitrile, and C 200 mM NH₄FA aqueous buffer; pH 4.5. Flow rate was 0.2 mL/min, separation temperature 40 $^{\circ}$ C. The isocratic mobile phase contained 20% acetonitrile and 40 mM NH₄FA buffer, pH 4.5. The buffer was prepared by dissolving 12.6 g of ammonium formate in 900 mL of water and adjusting pH to 4.5 with FA (99%); the volume was then brought to 1 L. The SCX experiment was carried out at 30 $^{\circ}$ C with flow rate 0.2 mL/min. Mobile phase A was water, B acetonitrile, and C 400 mM NH₄FA aqueous buffer, pH 3.25. The gradient was from 10 to 75% C in 40 min; pump B was used to deliver isocratically 25% acetonitrile for the entire duration of the salt gradient. The NH₄FA buffer was compatible with direct MS detection.

The MS conditions were as follows: capillary voltage 3.2 kV, cone voltage 30 V, extractor 1 V, and rf lens 0.3 V. Source temperature was set to 100 $^{\circ}$ C, desolvation to 350 $^{\circ}$ C. Desolvation gas flow was set to 350 L/h, cone gas to 50 L/h. MS scan span was 300–2500 *m/z*, scan time 2.2 s with 0.1-s interscan time. Spectra were collected in positive ESI mode.

Peptide Sample. Five protein (enolase, ADH, phosphorylase *b*, hemoglobin, BSA) tryptic digests including six nontryptic peptides (Rasg-1, angiotensin 1–7, bradykinin, angiotensin 2,

(17) Gilar, M.; Olivova, P.; Daly, A. E.; Gebler, J. C. *J. Sep. Sci.* In press.

(18) Gray, M.; Dennis, G. R.; Wormell, P.; Shalliker, R. A.; Slonecker, P. *J. Chromatogr. A* **2002**, 975, 285–297.

angiotensin 1, renin substrate, melittin) were included in the study. The theoretical number of peptides present in the mixture was 320, including the nontryptic peptides and 6 prominent miscleaved peptides. When short tryptic peptides (1–3 amino acids) are excluded, only 243 peptides should be detectable. Some of those were highly hydrophilic in nature and eluted in the void volume in RP-LC. Other peptides had poor intensity in ESI-MS and were not detected in some of the LC–MS modes. Only the most intense peptides common for *all* LC–MS experiments were considered in this study (196); therefore, the different LC modes were accurately compared using an identical data set. The average peptide length was 10.1 amino acids; the largest peptide was 37 amino acids long. The set comprised 1 singly charged, 130 doubly charged, 55 triply charged, 7 quadruply charged, and 3 peptides carrying five positive charges (at pH 3).

Data Analysis. MS data were processed with MassLynx software (Waters). Retention times of peptides were recoded manually according to their mass (extracted SIR MS chromatogram) and entered into MS Excel. The retention data normalization and calculation of peptide distribution between 2D separation space bins were carried out in MS Excel.

RESULTS AND DISCUSSION

2D Peptide Retention Time Plots. The peak capacity in 2D separations (P_{2D}) is described by eq 1 and can be calculated as

$$P_{2D} = P_1 P_2 \quad (1)$$

multiplication of peak capacities of both separation dimensions (P_1 , P_2).

This definition is valid only when the selectivity of separation is completely independent, and the entire 2D separation space is randomly populated by the peaks.¹³ Understandably, this condition is rarely fulfilled, limiting the practical peak capacity N_p of the 2D separations. Several 2D-LC schemes for separation of peptides have been suggested; however, the information about orthogonality of chosen LC modes for peptide separation is largely unknown.^{1,19} To evaluate the orthogonality of selected LC modes, we constructed the peptide retention maps, as described previously.¹⁷ Briefly, five protein digests (each comprising 20–100 peptides) were sequentially injected on the LC–UV–MS system, the peptides were identified by their unique mass, and their retention was recorded. Retention data were acquired for each LC mode in single-dimensional LC setup and normalized according to eq 2. RT_{\max} and RT_{\min} represent the retention times of the most

$$RT_{i(\text{norm})} = \frac{RT_i - RT_{\min}}{RT_{\max} - RT_{\min}} \quad (2)$$

and least retained peptide in the data set, respectively. The retention times RT_i are converted to normalized $RT_{i(\text{norm})}$; the values of $RT_{i(\text{norm})}$ range from 0 to 1. The normalization serves two purposes: First, it allows for comparison of different chromatographic data in a uniform 2D retention space, regardless of absolute retention time values. Second, it removes the void spaces

in the 2D separation plot, where no peaks elute. The voids can be caused by column void volume, by LC system gradient delay, or by using gradient spanning outside of the useful range (for example, gradient of 0–100% acetonitrile in RP-LC, while practically all tryptic peptides elute within 0–50% acetonitrile).

Normalized 2D plots (Figure 1) were constructed for an identical set of 196 peptides ranging in length from 4 to 37 amino acids (see Experimental Section). We first utilized the plots to evaluate the separation orthogonality. The impact of orthogonality on practical peak capacity and other aspects of 2D-LC separation (mobile phase compatibility) will be discussed later.

Orthogonality of Selected 2D-LC Systems. The Atlantis dC₁₈ column, operated under conditions suitable for proteomic LC–MS/MS experiment, was used to generate the basic set of retention time data. This data set in essence represents a common second dimension of 2D-LC. Plots in Figure 1 show correlations of Atlantis dC₁₈ data with another six LC modes. Examples of chromatograms are in Figure 2.

Figure 1A illustrates that the combination of two different types of RP columns provides only a limited orthogonality. The differences in selectivity between C₁₈ and Phenyl columns may be suitable for some applications, such as peptide mapping (Phenyl may resolve some critical peptide pairs),^{20–22} but they are not useful for 2D-LC applications. Other evaluated RP stationary phases show similar trends; the most distinct selectivity was observed for PFP sorbent (Figure 1B). However, the orthogonality is still limited and most of the 2D space is not used for separation.

An alternative approach was also evaluated, using RP-RP sorbents with a different pH of mobile phase in first and second separation dimensions^{17,23} (Figure 1C). It appears that pH is a more potent tool for altering the selectivity of separation in RP mode than the type of RP stationary phase (at least for charged solutes). Peptides in Figure 1C were divided into the three groups according to their pI to illustrate the separation mechanism. Acidic peptides are more retained at low pH, while basic peptides are retained at high pH. The selectivity of separation varies with pH for the “neutral” peptides (pI 5.5–7.5) as well. This is due to the fact that their net charge may also be affected by the pH, since the pK_a values of ionizable amino acids functional groups are between pH 3 and 10. The degree of orthogonality was evaluated for LC systems of pH 2.6 versus 7.8, 8.5, or 10; Figure 1C represents the most successful 2D-LC system obtained for the greatest pH difference. Although the pH-dependent selectivity changes were expected, the achieved degree of orthogonality is rather surprising. Since the C₁₈ sorbents were used in both separation dimensions, the orthogonality is mostly due to the pH effect.

Some authors have investigated the SEC utility for 2D-LC of peptides.²⁴ Because of a limited efficiency of SEC, we connected three columns in series to enhance the peak capacity and recorded the retention data. The SEC chromatogram is shown in Figure 2D; the retention time map is in Figure 1D. The residual interaction of relatively hydrophobic peptides with the sorbent

(20) Chloupek, R. C.; Hancock, W. S.; Marchylo, B. A.; Kirkland, J. J.; Boyes, B. E.; Snyder, L. R. *J. Chromatogr., A* **1994**, 686, 45–59.

(21) Hancock, W. S.; Chloupek, R. C.; Kirkland, J. J.; Snyder, L. R. *J. Chromatogr., A* **1994**, 686, 31–43.

(22) Guo, D. C.; Mant, C. T.; Hodges, R. S. *J. Chromatogr.* **1987**, 386, 205–222.

(23) Toll, H.; Oberacher, H.; Swart, R.; Huber, C. G. *J. Chromatogr., A* **2005**, 1079, 274–286.

(19) Gygi, S. P.; Rist, B.; Gerber, S. A.; Turecek, F.; Gelb, M. H.; Aebersold, R. *Nat. Biotechnol.* **1999**, 17, 994–999.

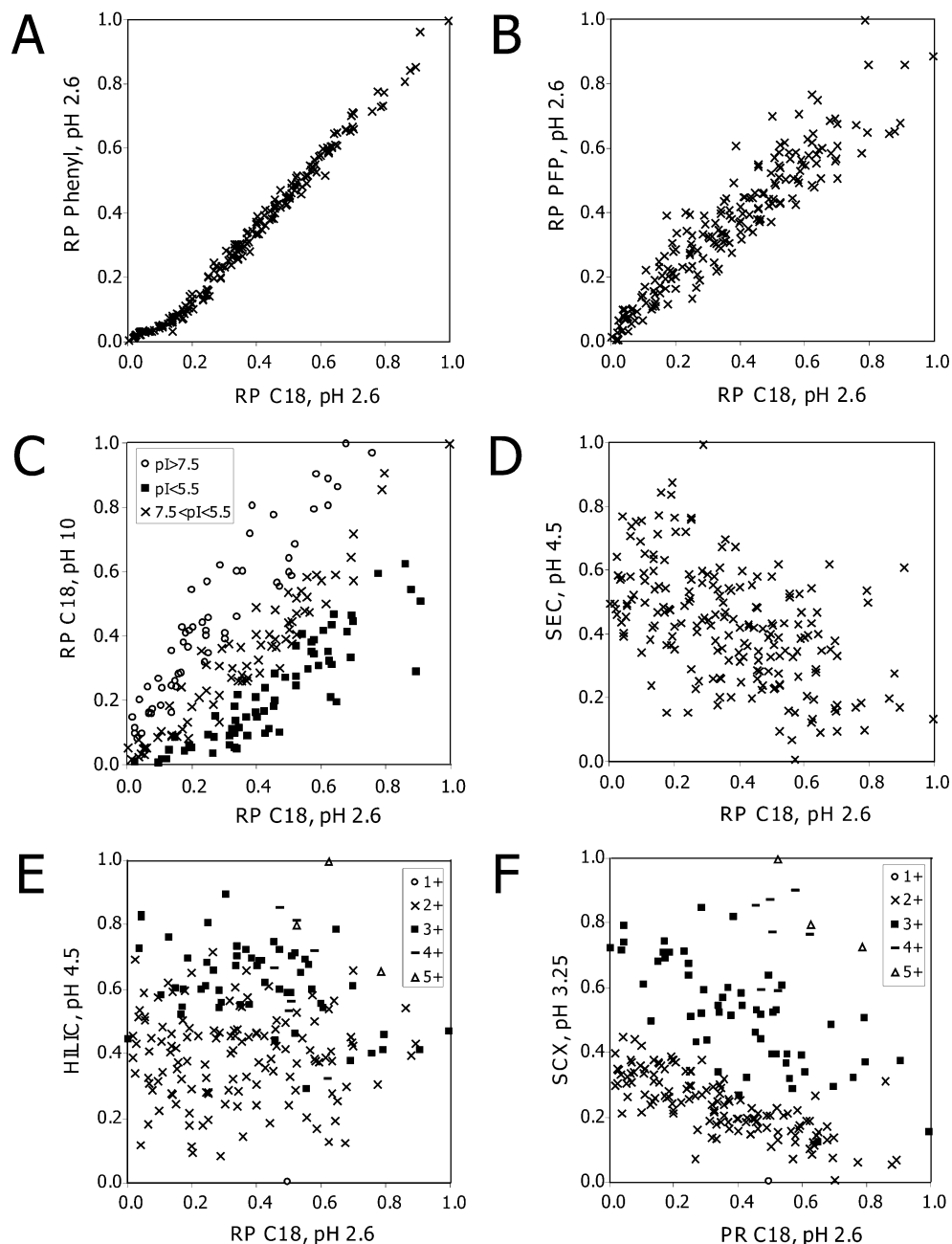


Figure 1. Normalized retention time plots for selected 2D-LC systems.

was minimized by addition of 20% acetonitrile and 40 mM NH_4FA buffer, pH 4.5 into a mobile phase. However, some secondary interaction still prevailed, limiting the recovery of larger peptides and affecting the overall selectivity of separation. Only a loose correlation between size of the peptides and their SEC retention was observed. Longer peptides (more hydrophobic and therefore more retained in RP mode) elute earlier in SEC, as expected. However, the degree of orthogonality for the RP \times SEC combination is greater than one may expect (Figure 1D). This behavior is likely to be caused by the peptide secondary interaction with the sorbent, as mentioned above.

HILIC mode was also evaluated for peptide separation. Only a few reports have been published for peptide separation in HILIC mode, mostly using polyaspartate²⁵ or amide sorbents.²⁶ We have utilized a HILIC column packed with bare silica sorbent; both peptide peak shapes and recovery were good (see chromatogram in

Figure 2E). No precipitation was observed when dissolving peptide samples in 70% acetonitrile prior to injection. Figure 1E illustrates a high degree of orthogonality for the HILIC-RP 2D-LC system. Some correlation between peptide charge and their HILIC retention suggests that the retention mechanism includes both partitioning and ionic interaction (due to the charged silanols²⁷). Therefore, the separation selectivity partially resembles the peptide retention in SCX mode (Figure 1F). The high degree of HILIC-RP system orthogonality makes it a promising approach for 2D-LC.

Since the SCX-RP combination represent a most common approach to 2D-LC of peptides, we have investigated the SCX

(24) Opiteck, G. J.; Jorgenson, J. W.; MacNair, J. E.; Moseley, M. A., 3rd. *Anal. Chem.* **1997**, 69, 2283–2291.

(25) Alpert, A. J. *J. Chromatogr.* **1990**, 499, 177–196.

(26) Yoshida, T. *Anal. Chem.* **1997**, 69, 3038–3043.

(27) Zhu, B. Y.; Mant, C. T.; Hodges, R. S. *J. Chromatogr.* **1991**, 548, 13–24.

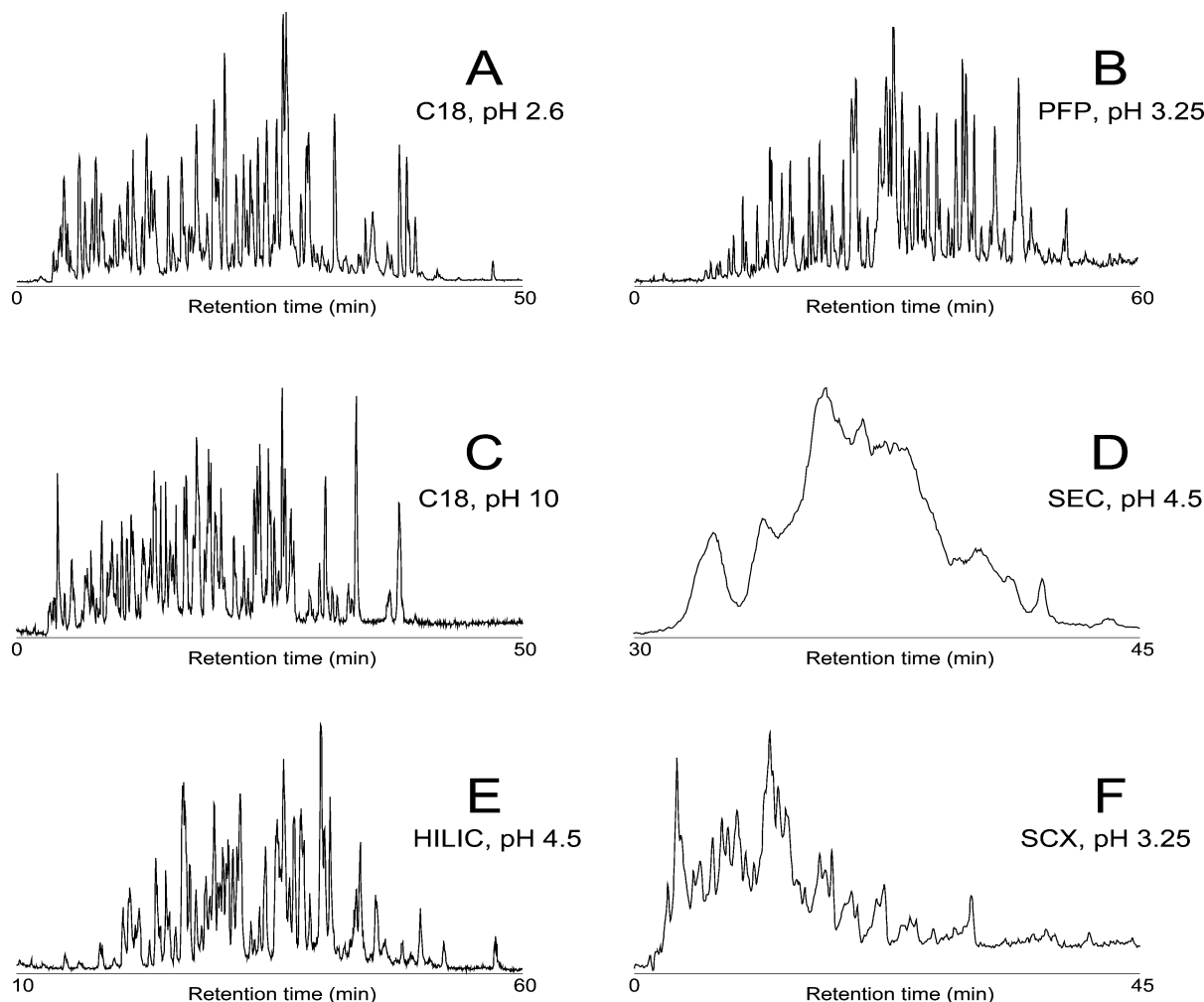


Figure 2. LC–MS chromatograms of phosphorylase *b* tryptic digest using selected LC modes. (A) C18, pH 2.6; (B) PFP reversed phase; (C) C18, pH 10; (D) SEC; (E) HILIC; (F) SCX. The digest comprises ~100 peptides.

sorbents in greater depth.¹⁷ Elution in SCX mode is usually accomplished with a gradient of NaCl, which makes this mode incompatible with MS detection. Both off-line and on-line 2D-LC–MS setups usually rely on sample desalting, often realized via RP trapping columns.²⁸ The published reports indicate that available SCX sorbents exhibit a secondary (hydrophobic) interaction, which reduces the recovery of hydrophobic peptides.²⁹ It has been suggested that addition of organic solvents in a mobile phase improves the peak shape and peptide recovery. However, even with 25% acetonitrile in the mobile phases, we observed a lower number of peptides than expected.¹⁷ Therefore, we investigated the possibility to carry out the SCX experiment with alternative mobile phases and direct MS detection.

The mobile phase was prepared from volatile buffer, namely, 400 mM ammonium hydroxide titrated to pH 3.25 with FA. The final concentration of FA was ~1.3 M (5% FA). Since the pK_a of FA is 3.75, the pH of buffer (0.5 pH unit lower) ensures that only 25% of the FA is deprotonated, bringing the concentration of $[H^+]$ to 325 mM. Together with the ammonium cation, the total cation strength of this buffer adds up to 725 mM. The gradient from 10 to 75% buffer (72.5–543.75 mM) successfully eluted all desirable

peptides up to 5+ charge. The MS signal was not dramatically suppressed (MS chromatogram see in Figure 2F); on-line LC–MS detection was possible. The retention time 2D plot is shown in Figure 1F.

As expected, the SCX selectivity is driven by peptide charge.^{27,29} Trends emerging from the plot suggest that peptide retention depends also on its length. The large peptides (that are more hydrophobic and better retained in RP) are relatively less retained in SCX chromatography compared to short peptides of the same charge. This behavior implies that charge density (which is greater for the shorter peptides) plays a secondary role in the retention mechanism. We believe that the charge density is responsible for the ability of SCX sorbent to resolve peptides with the same charge rather than the residual hydrophobic interaction of the peptides with sorbent.³

The orthogonality of the SCX-RP combination appears to be good. However, one may notice that the most abundant groups of peptides (66% peptides are 2+ charged; 28% peptides are 3+ charged) form tight clusters (Figure 1F). The 2D separation space is not covered with the data points uniformly; therefore, the orthogonality is lower than anticipated.

Geometric Description of Orthogonality. The tools developed for a characterization of orthogonality in 2D-LC separation

(28) Vollmer, M.; Horth, P.; Nagele, E. *Anal. Chem.* **2004**, *76*, 5180–5185.

(29) Alpert, A. J.; Andrews, P. C. *J. Chromatogr.* **1988**, *443*, 85–96.

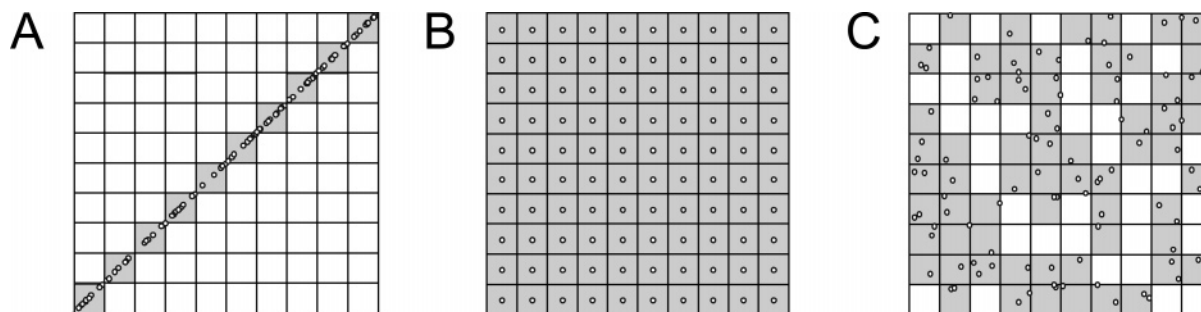


Figure 3. Geometric orthogonality concept. Hypothetical separation of 100 analytes in 10×10 normalized separation space. (A) Nonorthogonal system, 10% area coverage represents 0% orthogonality. (B) Hypothetical ordered system, full area coverage. (C) Random, ideally orthogonal, system, area coverage is 63% representing the 100% orthogonality.

utilize several complementary descriptors, such as informational similarity, percentage of synentropy, peak spreading angle, and practical peak capacity.^{14,15,18} While those mathematical models are suitable for description for situations presented in Figure 1A–C, the orthogonality of retention maps in Figure 1D and E and especially in Figure 1F (data clusters) may be difficult to describe. Therefore, we developed a simple geometric approach for characterization of data orthogonality with an intuitive, single descriptor. The model utilizes the following approach: (i) The normalized retention data (eq 2) are plotted into a 2D separation space as shown in Figure 1. (ii) Area is assigned to each data point, representing a normalized peak area (peak width is measured according to Snyder at 4σ , at 13.4% of peak height.^{9,10}) (iii) The orthogonality is defined as a normalized area covered by peaks in 2D separation space. The greater coverage, the greater is the orthogonality.

This proposed geometric approach has several potential difficulties. It is not trivial to calculate a multiple area intersection of closely eluting peaks in order to calculate a net area covered by peaks. In the case when the peak capacity (peak width) is not the same in both dimensions, the 2D peak area assumes an elliptical shape, which further complicates the mathematical solution.³⁰ In addition, the area coverage changes with the number of data points, which undermines the orthogonality comparison for different data sets. Finally, the average peak width in gradient chromatography changes with the separation conditions, such as gradient slope, further reducing the generality of the proposed approach. Therefore, further assumptions were made to simplify the problem: (i) 2D separation space was divided into rectangular bins, similar to those in earlier published reports. Each bin then corresponds to a peak area. (ii) The data set is superimposed with a separation space divided into the number of rectangular bins that equal the number of data points. In other words, the peak capacity of normalized 2D separation space is equal to the number of separated components. Therefore, the data sets of different sizes can be compared. (iii) The area of all normalized bins containing data points is summed. The degree of area coverage describes an orthogonality of an interrogated 2D separation system.

Figure 3 further illustrates the geometric approach to orthogonality description. The plots represent 2D separation space with peak capacity of 100 (peak capacity in both dimensions is 10) populated by 100 data points. In the case when the separation selectivity on both dimensions is identical (completely nonorthogonal 2D system), the data points are lined up along the

diagonal, and the surface coverage is 10% (Figure 3A). One can also imagine an extreme case, when all data points fall within a single bin (surface coverage of 1%). This can happen only if the separation completely fails in both dimensions and all components elute as a single peak. This case does not have a practical importance and is not considered.

Figure 3B illustrates another extreme case. The data set is evenly distributed throughout the separation space, covering 100% of the surface. This situation is hypothetical, describing an idealized separation system. Figure 3C represents a more realistic case with a randomized data set. Some bins contain more than a single data point (coeluting peaks), while other separation space is unused. From the theory of overlap in 2D separations, one can calculate the average area used for separation.³⁰ For the system where the number of analytes m is being separated in 2D separation space with the same peak capacity P_{2D} , the surface coverage is an average 63%. The mathematical solution was described for spherical and elliptical spots,³⁰ assuming that the separation is accurately described by Poisson statistics. In this work, we use rectangular spots (bins), but the same degree of coverage is expected, because the overlap probability depends on the spot area rather than shape. However, an additional assumption is used in present work; instead of rigorously calculating the area covered by eluting peaks taking into account the numerous bin intersections, we simply sum the number of bins containing the data points (Figure 3).

To verify that the approach used is an acceptable simplification, we carried out multiple simulations. In the data sets, 196 data points were randomly distributed in a normalized 2D space divided into 14×14 bins (total peak capacity of 196), and the bins containing peaks were summed. Simulations carried out in an unbound space³⁰ reveal that the area coverage is an average 63%, a good agreement with analytical solution. The simplistic approach provides a useful and reasonably accurate estimate of area utilized in 2D separations. Most importantly, this approach is applicable for area description of nonorthogonal (nonrandom) experimental 2D-LC results, where the statistical theory of overlap is not applicable.³⁰

As explained above, the surface used for 2D separation varies from 10 (nonorthogonal system) to 63% (ideally orthogonal separation). This represents a practical range of orthogonality O , defined by eq 3. Σbins is the number bins in 2D plot containing

$$O = \frac{\Sigma \text{bins} - \sqrt{P_{\max}}}{0.63P_{\max}} \quad (3)$$

(30) Davis, J. M. *J. Sep. Sci.* **2005**, *28*, 347–359.

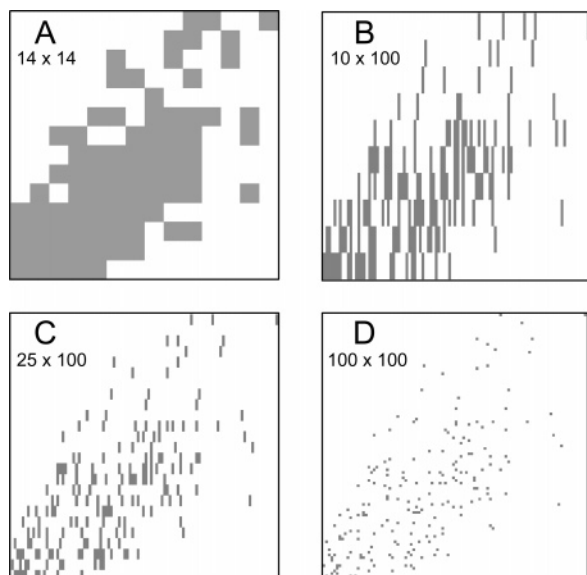


Figure 4. Impact of 2D-LC system peak capacity on the peptide separation. Normalized separation space was divided into (A) 14×14 , (B) 10×100 , (C) 25×100 , and (D) 100×100 bins representing the peak capacity of the hypothetical LC separation dimensions. Number of observed bins is summarized in Table 3.

data points, and P_{\max} is total peak capacity obtained as a sum of all bins. For the rectangular separation space (peak capacity is the same in both dimension, $P_1 = P_2$), the P_{\max} can be calculated as P^2 ; then the $\sqrt{P_{\max}}$ value is equal to the number of bins intersected by a diagonal line (see, for example, Figure 3A). The orthogonality values range from 0 to 1. When expressed as orthogonality percent ($O\%$), the systems in Figure 3A and Figure 3C are 0 and 100% orthogonal, respectively.

The orthogonality of 2D-LC systems shown in Figure 1 was calculated according to eq 3. The normalized retention data of 196 peptides were plotted in a space of 14×14 bins (total peak capacity of 196 bins). The distribution of data points in 2D separation space was calculated in MS Excel. The graphical example of solution for high-/low-pH RP-RP system in Figure 1C

is shown in Figure 4A. The numbers of bins used for separation for all six 2D-LC systems in Figure 1 are given in Table 1. The calculated orthogonality values are also shown (as orthogonality %). As one would expect from retention plots in Figure 1, the best orthogonality was obtained for HILIC-RP 2D-LC system. About 51% of separation area is covered by eluting peptides; the system is therefore 69% orthogonal. Interestingly, the orthogonality of SCX-RP and RP-RP 2D-LC systems are practically identical (54 and 53%, respectively).

The results illustrate the fact that it is unrealistic to assume that 2D-LC system currently used for separation of peptides provides an ideal orthogonality. The question remains, what is the impact of nonideal orthogonality on the practical peak capacity in 2D separations.

Practical 2D-LC Peak Capacity. Several practical considerations limit the achievable peak capacity in 2D-LC. The orthogonality of separation is important, as well as peak capacities in both LC dimensions. Because the proteomic 2D-LC separations are often performed in capillary- or nano-LC modes (more sensitive to extracolumn contributions to peak broadening), the peak capacity is typically lower than in analytical LC scale. Second, the sample transfer from first to second dimension is complicated by the solvent compatibility and practical fraction volume. Incompatible mobile phases can induce peak broadening in second dimension or a sample breakthrough. In addition, the trapping columns used in the nano-LC setup further complicate the 2D-LC setup (relative retentivity, void volume, and total gradient delay have to be considered). A discussion of those parameters is beyond the scope of this paper. The following discussion concentrates on the orthogonality and its impact on 2D-LC practical peak capacity (N_p).

Figure 1A illustrates the 2D-LC system with a poor orthogonality (C18 versus Phenyl). Understandably, the number of peaks resolved in this system will be lower than in a more orthogonal 2D-LC setup shown in Figure 1E (HILIC versus RP). The theoretical peak capacity (eq 1) is comparable, but practical peak capacity is dramatically different. A practical peak capacity can be derived from the proposed geometric model, using the

Table 1. Number of Area Bins Used for Separation and Orthogonality (%) for Investigated 2D-LC Systems

	Atlantis C18, pH 2.6	Phenyl, pH 2.6	XTerra C18, pH 10	HILIC, pH 4.5	SEC, pH 4.5	SCX, pH 3.25	PFP, pH 3.25
Number of Bins Used for Separation ^a							
Atlantis C18, pH 2.6	14	30	80	100	86	81	52
Phenyl, pH 2.6	30	14	84	99	81	82	54
XTerra C18, pH 2.6	80	84	14	87	88	82	75
HILIC, pH 4.5	100	99	87	14	78	81	95
SEC, pH 4.5	86	81	88	78	14	75	83
SCX, pH 3.25	81	82	82	81	75	14	81
PFP, pH 3.25	52	54	75	95	83	81	13
Orthogonality (%) ^b							
Atlantis C18, pH 2.6	0	13	53	69	58	54	31
Phenyl, pH 2.6	13	0	56	69	54	55	32
XTerra C18, pH 2.6	53	56	0	59	60	55	49
HILIC, pH 4.5	69	6	59	0	52	54	65
SEC, pH 4.5	58	54	60	52	0	49	56
SCX, pH 3.25	54	55	55	54	49	0	54
PFP, pH 3.25	31	32	49	65	56	54	-1

^a Separation space was divided into 196 area bins (14×14). ^b Orthogonality was calculated from eq 3 and expressed as %. The values vary approximately between 0 and 100% (on-orthogonal to ideally orthogonal 2D-LC system). The -1% value for the PFP \times PFP system means that peptides are not evenly distributed over PFP 1D separation space; one diagonal bin did not have any data.

Table 2. Practical Peak Capacity Estimate for Selected 2D-LC Modes

	Atlantis C18, pH 2.6	1D-LC System XTerra C18, pH 10	SCX, pH 3.25	HILIC, pH 4.5	SEC, pH 4.5
peak width $w_{13.4\%}$ (4σ) ^a	0.35	0.35	0.6	0.4	1
effective anal. time t_g (min) ^b	40	40	30	31	13
1D peak capacity P^c	115	115	51	79	14

	C18, pH 10 × C18, pH 2.6	2D-LC System SCX × C18, pH 2.6	SCX × HILIC	HILIC × C18, pH 2.6	SEC × C18, pH 2.6
theoretical P_{2D}^d	13291	5880	4029	9050	1610
surface coverage fraction ^e	0.41	0.41	0.41	0.51	0.44
practical peak capacity N_p^f	5425	2430	1652	4616	708

^a Peak width measured at 13.4% peak height. ^b analytical time between first and last eluting peak. ^c calculated as $P = 1 + t_g/w_{13.4\%}$. ^d calculated from eq 1. ^e calculated as $\sum \text{bins}/P_{\text{max}}$. ^f calculated from eq 5.

knowledge of 2D surface coverage (eq 4). Practical peak capacity

$$N_p = P_{2D} \frac{\sum \text{bins}}{P_{\text{max}}} \quad (4)$$

N_p is lower than the theoretical peak capacity P_{2D} defined by eq 1, because only a fraction of the surface is utilized for separation. Combining eqs 1 and 4, the N_p can be expressed as eq 5. Equation

$$N_p = P_1 P_2 \frac{\sum \text{bins}}{P_{\text{max}}} \quad (5)$$

5 illustrates the impact of peak capacities of both separation dimensions on the practical peak capacity in 2D. The calculation of N_p for selected 2D-LC systems is illustrated in Table 2; peak capacities of 1D-LC modes were estimated from an average peak width of peptides and the retention time window as described earlier.¹² The peak capacity of selected LC modes can also be visually appreciated in Figure 2.

Table 2 illustrates the importance of peak capacity on several examples. The RP-RP 2D-LC system provides the greatest practical peak capacity, although its orthogonality is lower than the HILIC-RP system. The orthogonality of RP-RP and SCX-RP systems is nearly identical, but the latter system has lower N_p , due to the lower SCX peak capacity. The SEC-RP system exhibits a good orthogonality, but low SEC peak capacity undermines the usefulness of this system for 2D-LC analysis.

The practical peak capacity calculated from eq 5 assumes a frequent fraction collection in first dimension (with narrower fractions than the typical peak width). While the fraction oversampling is important to maintain the component resolution in the 2D chromatogram,³¹ it also spreads the peptides in many fractions, reducing their ultimate concentration and MS detection limit. MS signal and time of analysis are the primary concerns in a proteomic experiment. In a typical experiment, the number of collected fractions is often limited,²⁸ sacrificing the overall peak

capacity. For example, when collecting 10 fractions in the first LC dimension, its peak capacity is reduced to 10, even if the theoretical peak capacity is 100. The practical peak capacity values calculated from eq 5 are therefore reduced.

The impact of fraction collection frequency on the peptide resolution is illustrated in Figure 4. Figure 1A shows the 2D-LC separation of 196 peptides plotted in the 14×14 2D separation space (peak capacity is 14 in both dimensions). The bins with eluting peptides are highlighted in gray. Figure 4A represents the example of setup utilized for orthogonality calculations (Table 1). Another three plots in Figures 4B–D show how the separation improves when using more frequent fraction collection in the first dimension (10, 25, and 100 fractions; theoretical peak capacity is 100 or higher); the RP column in the second dimension has fixed peak capacity ($P = 100$). The number of overlapping (adjacent) bins decreases for the systems with greater peak capacity. The numbers of observed bins are summarized in Table 3.

The frequency of fraction collection is an important consideration for proteomic experiments. When using a fraction collection window equal to or smaller than the average peak width, all peptides are divided in two or more fractions with the consequences on the peptide concentration and overall 2D-LC analytical time. On the other hand, a wide collection window (less frequent fraction collection) undermines the 2D-LC resolution.

Other Considerations for 2D-LC. Two basic approaches are used for 2D-LC separation in proteomic research. When mobile phase permits, the fractions may be transferred on-line from first to second dimension. An example of an on-line approach is SCX-RP 2D-LC. The salt steps or gradients with increasing ionic strength are used to elute peptides from the first SCX dimension and transfer onto the second RP dimension. Some researchers favor this approach due to ease of use and minimal sample manipulation.^{1,28,32} However, it has been noted that SCX sorbents suffer from nonspecific interaction, presumably due to a residual hydrophobicity. Hydrophobic peptides may be incompletely recovered or eluted with a poor peak shape.²⁹ The addition of organic solvent in a SCX mobile phase has been recommended

(31) Murphy, R. E.; Schure, M. R.; Foley, J. P. *Anal. Chem.* **1998**, *70*, 1585–1594.

(32) Wolters, D. A.; Washburn, M. P.; Yates, J. R., 3rd; Wolters, D. *Anal. Chem.* **2001**, *73*, 5683–5690.

Table 3. Resolution of 196 Peptides in 2D-LC Separation Space Depending on First and Second Dimension Peak Capacity^a

	2D-LC peak capacity			
	14 × 14	10 × 100	25 × 100	100 × 100
number of bins containing peptides	80	159	182	193
bins containing more than 1 peptide	48	32	14	3
bins containing only 1 peptide	32	127	168	190

^a The y-axis represent first LC dimension peak capacity (number of collected fractionations). See also Figure 4.

to correct the problem, but the organic solvents interfere with on-line fraction transfer to a second RP dimension.

The off-line SCX-RP 2D-LC setup utilizes a fraction collection and offers a greater flexibility than the on-line setup. Restrictions of mobile-phase compatibility between first and second separation dimensions are relaxed; 25% acetonitrile is often used in SCX mobile phases, followed by organic content reduction by partial evaporation.³

The majority of LC modes investigated in this work use solvents that are not directly compatible. The 2D-LC setup is therefore limited to off-line approach. We have successfully used a partial fraction evaporation for fractions collected from high-pH RP-LC; after the organic content reduction, the fractions were injected in a second low-pH RP separation dimension without noticeable peak distortion.¹⁷ The peptide solubility in the high-pH mobile phase was good; however, to eliminate possible chemical modification, we stored the samples in neutral pH. The fractions were evaporated or neutralized within 1 h after 1D-LC collection. No peptide loss was detected observing those rules.

In the HILIC experiment, good peak shape and recovery were obtained (peptides were dissolved in 70% acetonitrile) when using bare silica-based sorbent. Interestingly, no on-column precipitation and no carryover were observed. Since the HILIC is compatible with MS detection, it could represent as attractive option for the second chromatographic dimension. Recent reports note a significantly better LC-MS sensitivity for highly polar compounds for HILIC with highly organic mobile phases.³³ However, we did not detect any improvements of MS signal for peptides over RP-LC.

The loss of peptides was observed in SEC mode. The SEC diol sorbent with 60-Å pore size was used for the separation, rather than 125-Å sorbent as described elsewhere.²⁴ The pore size is more adequate for separation of peptides, but the excess of available surface reduces the peptide recovery, apparently due to nonspecific adsorption. Ammonium formate aqueous buffer (40 mM) with 20% acetonitrile had to be used to minimize the peptide interaction with the sorbent. When lower ionic strength and acetonitrile content were used in the mobile phase, some peptides eluted outside of the total inclusion window, while hydrophobic peptides did not elute at all.

A major limitation of SEC is low peak capacity. Three columns connected in series provide only a moderate peak capacity ($P = 14$). Only a small portion of analysis time was used for the separation (inclusion window), which further undermines the utility of SEC for a 2D-LC approach.

In this work, we used SCX with a LC-MS-compatible volatile mobile phase. Contrary to our earlier report,¹⁷ all peptides of interest (including the hydrophobic ones) were detected in this work (with 25 or 5% of acetonitrile in the mobile phase; 5% ACN data not shown). This raises a question about the mechanism of peptide loss in SCX. Either the peptides are incompletely eluted from the SCX column (with NaCl eluent), despite the acetonitrile content in the mobile phase, or some postcollection precipitation occurs in the presence of a high concentration of nonvolatile salts. We believe that LC-MS-compatible buffers offer benefits for SCX fractionation of peptides.³⁴

CONCLUSIONS

The results presented in this paper allow for several general conclusions.

1. No separation mode in 2D-LC is likely to offer a complete orthogonality of separation; rather than theoretical, the practical peak capacity of 2D separation systems should be used, taking into consideration also the number of collected fractions.

2. A proposed geometric approach, using the degree of surface coverage with peaks, can simply describe an orthogonality of any 2D-LC or 2D separation scheme.

3. 2D-LC based on the RP-RP using a different pH in both dimensions has an orthogonality comparable to the most common 2D-LC approach utilizing the combination of SCX and RP LC modes. This may have a significant impact on the practice of performing multidimensional proteomic analysis. Another investigated 2D-LC approach, based on HILIC-RP, provides a greater degree of orthogonality. However, its utility may be hindered by poor solubility of peptides in high organic content solvents.

4. The benefits of a highly efficient separation in the first dimension are most apparent when a larger number of fractions is collected. However, this increases the pressure on a sample throughput in a second separation dimension.

ACKNOWLEDGMENT

The authors thank Aleksander Jaworski for helpful suggestions for the manuscript.

Received for review May 26, 2005. Accepted July 27, 2005.

AC050923I

(33) Naidong, W.; Eerkes, A. *Biomed. Chromatogr.* **2004**, *18*, 28–36.

(34) Man, P.; Novak, P.; Cebecauer, M.; Horvath, O.; Fiserova, A.; Havlicek, V.; Bezouska, K. *Proteomics* **2005**, *5*, 113–122.